Diffusion and Reaction in Whole Wheat Grains during Boiling

A. G. F. Stapley and P. J. Fryer
School of Chemical Engineering, University of Birmingham, Birmingham, B15 2TT, U.K.

L. F. Gladden
Dept. of Chemical Engineering, University of Cambridge, Cambridge, CB2 3RA, U.K.

The boiling of whole wheat grains was studied using magnetic resonance imaging (MRI) and pulsed-gradient-spin-echo nuclear magnetic resonance (NMR) (PGSE NMR). MRI was used to image moisture distributions across a central section of grains boiled for different times at either 100 or 120°C. A moisture front gradually moved into the grain, although some moisture did penetrate ahead of the front. PGSE NMR, which measures self-diffusion, indicated that two pools of water with differing diffusion characteristics may exist within the grain. Diffusion models suggested from the PGSE results were incorporated into finite-element simulations along with the Thomas-Windle model for diffusion/relaxation in polymers. Simulation results were compared to the MRI data, and the best fit was achieved using the Thomas-Windle model with a step-change in diffusivity above a critical moisture content. This behavior is similar to that of diffusion in polymers undergoing a glass transition, a phenomenon widely accepted to occur when starch gelatinizes.

Introduction

Starch and wheat grains

Starch is the world's most important food energy source, being the major component of cereal grains and tubers. In order to be fully digestible, it must first be gelatinized by hydrating and heating. The heat/moisture treatment is usually effected by one of two routes:

(i) Grind into a flour, mix the flour with water and other ingredients to form a dough, which is then heated (that is, baked). This is done for cereal grains only.

(ii) Steam or boil the intact grain or tuber. In the case of tubers (such as potato) where water is already present in large quantities inside the tuber, cooking is limited by the transfer of heat into the tuber. However, for cereal grains gelatinization relies on the diffusion of water into the grain since grains must be stored at low moisture contents to prevent microbial growth and germination.

The choice of method is dependent on both the starch source, and on historical preference. For example, whereas rice and potatoes are cooked whole, the overwhelming majority of wheat is milled. The cooking of intact whole wheat grains is, however, industrially important in breakfast cereal manufacture (Miller, 1988). Grains are first contacted both with steam and boiling liquid water, typically by heating to ~ 140°C in a pressure cooker at 4 bara. The development of flavors is critically dependent both on the temperature and moisture content history of the material (for example, Yaylayan et al., 1992). After cooking, the grains are soft enough to be worked into the final breakfast cereal product. The initial cooking process underpins all subsequent operations. To produce a product of the desired quality at minimum cost, it is thus important to be able to optimize the cooking process. This requires an understanding of the engineering processes involved in cooking: the diffusion of water into the grain and the subsequent gelatinization of the starch within the grain into a digestible form.

Wheat grains have a complex construction (see Figure 1), but are basically composed of the starchy endosperm and the wheat germ (located at one end). The two are surrounded by a protective layer which acts to maintain grain integrity and prevent excessive ingress of water. The endosperm makes up

Correspondence concerning this article should be addressed to P. J. Fryer.

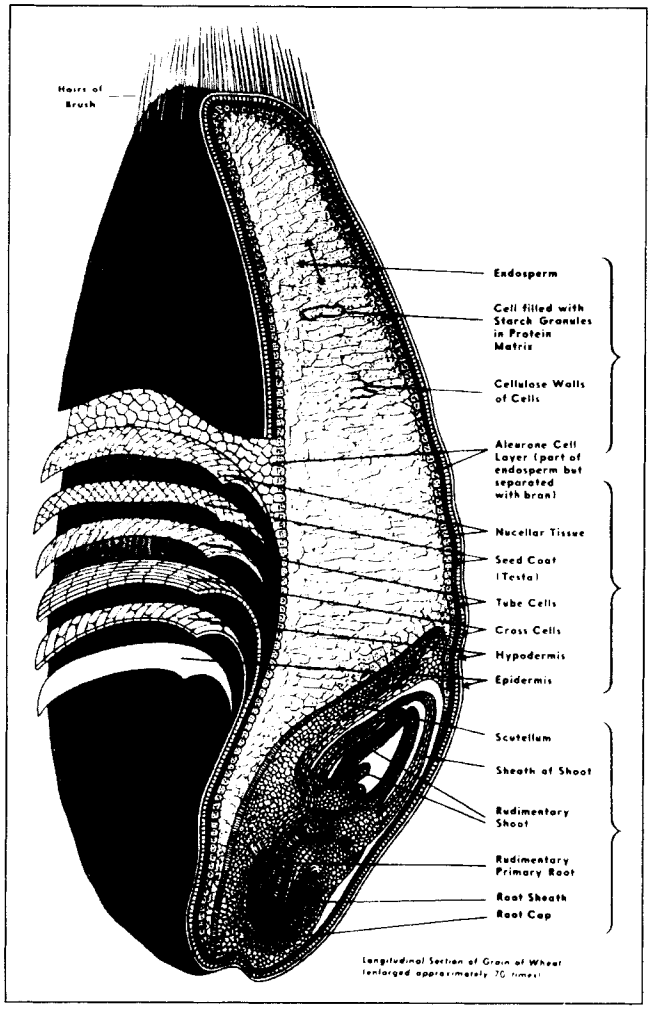

Figure 1. Anatomy of a wheat grain.

From Mattern (1991).

most of the grain (82% of the typical mass; Orth and Shellenberger, 1988), and is organized into starch granules (1–40 μm, see Jane et al., 1994) which are individually encased by a lipoprotein membrane (Galliard and Bowler, 1987), and embedded in a protein matrix (Stenvert and Kingswood, 1977). The wheat germ contains no starch (Mattern, 1991). Within the granule, amorphous starch alternates with mixed crystalline/amorphous regions over a length scale of 100–400 nm (Imberty et al., 1991; French, 1984; Blanshard, 1987). Two types of grain are generally classified: (i) "mealy" grains have a disordered endosperm structure with air spaces interspersed between the granules and protein bodies (Stenvert and Kingswood, 1977), and (ii) "vitreous" grains have a continuous, ordered starch protein matrix.

The structure of starch granules is complex, and the mechanisms associated with starch gelantinization are complicated. The interaction between water and starch has been extensively studied, and a vast literature now exists on the topic (Biliaderis, 1990; Levine and Slade, 1989). It is well established that the temperature at which starch conversion occurs decreases with increasing moisture content (Donovan, 1979; Eliasson, 1980). The precise mechanism of gelatinization, however, is still not fully understood, but it is generally accepted that there are two basic processes involved (Slade and Levine, 1988):

(i) A glass transition which affects the amorphous areas of the starch

(ii) Melting of starch crystallites.

In whole grain cooking, gelatinization is further complicated by a diffusional constraint, as water must diffuse into the grain for gelatinization to occur. The literature on whole grain cooking is small and devoted almost exclusively to rice (of the eleven articles found on grain cooking during this work, only one used wheat grains). The objective of this study is to analyze the cooking problem and develop an engineering model for the boiling of grains which can be applied to grain cookers. Unlike previous work on grain cooking, this model is based on direct experimental observation of the moisture profiles within grains using MRI, and direct measurement of the self-diffusion coefficient of water in the grain using the PGSE NMR.

Previous models of grain processing

Most previous work has used water uptake (gravimetric) measurements as the prime source of experimental data. These have been fitted to a number of simple models:

(i) Diffusion Equation. Fan et al. (1961) used a truncated form of the analytical solution for diffusion into spheres (Becker, 1959, 1960) to model water absorption in wheat up to 98°C. Plotting moisture gain vs. square root of the absorption period revealed reasonably linear relationships, although there was an initial rapid weight gain of approximately 2–4%, attributed to a rapid pickup of moisture by capillary action into the bran and germ. An Arrhenius plot of the extracted diffusion coefficients, however, showed two straight line fits to data (i) above 65°C and (ii) below 65°C. There was a significant increase in activation energy in the higher-temperature regime, attributed to the change in the wheat structure due to gelatinization and protein denaturation. Diffusivities of 2.46×10^{-10} $m^2\cdot s^{-1}$ and 1.41×10^{-10} $m^2\cdot s^{-1}$ were reported for the Ponca and Seneca varieties at a temperature of 98.3°C. This method was also employed by Bandyopadhyay and Roy (1976) for modeling absorption of water into rice, who also found an initial rapid increase in water content, and a nonlinear Arrhenius plot.

(ii) First-Order Reaction. Suzuki et al. (1976) adopted a kinetic approach to model cooking of presoaked rice. A simple first-order kinetic model adequately fitted the data. Again, an Arrhenius plot of the extracted rate constants showed two linear regions of different activation energies, here above and below 110°C. Subsequent studies using the same first-order kinetic model also found two linear regions (Cho et al., 1980; Juliano and Perez, 1986). The activation energy above 110°C was approximately half that of below 110°C. The authors suggested that the overall kinetics of cooking were governed by two processes: (i) diffusion of water from the grain exterior to the boundary of a central unreacted core, and (ii) reaction of water with starch at the boundary of the unreacted core. It was further suggested that below 110°C reaction is rate-limiting and above 110°C diffusion is rate-limiting.

(iii) "Cooking Core" Model. Suzuki et al. (1976) then developed a "cooking-core" model, analogous to the "unreacted core" model used in heterogeneous catalysis, where re-

action occurs at a front which gradually moves from the outside to the inside of a particle. The "reaction" term used was actually a mass-transfer term of water across the boundary between unreacted and reacted starch. Suzuki et al. (1977) modeled mass uptake data for both cooking and lower-temperature soaking of rice. The ratio of the diffusion and "reaction" resistances increased from less than 0.05 at 90°C to 0.4 at 98.5°C, suggesting again that diffusion becomes relatively more important at higher temperatures, corresponding to a greater increase in reaction rate with temperature.

(iv) Combined Diffusion and Reaction. In their study of rice cooking, Bakshi and Singh (1980, 1982) modeled parboiling using the Danckwerts (1950, 1951) equation, which combines the diffusion equation with a first-order reaction term

$$\frac{D}{r}\frac{\partial^2(rc)}{\partial r^2} - kc = \frac{\partial c}{\partial t} \tag{1}$$

Bakshi and Singh fitted Eq. 1 to experimental data; Arrhenius plots for diffusivity and reaction rate both showed discontinuities of slope at approximately 85°C. Similar arguments to those advanced by Suzuki et al. (1976, 1977) were used in explanation. The Danckwerts equation was also employed by Cabrera et al. (1984) for modeling the nixtamilization (alkali cooking) of corn kernels.

Activation energies for the diffusion coefficient of water in cooking grains from the above reports are summarized in Table 1. However, each model involves incorrect assumptions:

(i) Diffusion-only models do not account for starch conversion

(ii) Reaction-only models take no account of the diffusive resistance

(iii) The reactions involved are much more complex than a first-order scheme

(iv) Water does not become immobilized upon gelatinization of starch as is assumed in the Danckwerts equation

(v) Grains are not spherical.

The profusion of models means that there is no clear trend in the table. It is clear that the mechanisms of starch conversion and water diffusion cannot be determined from overall reaction and water uptake data.

Use of MRI to analyze diffusing systems

The above studies are largely based on gravimetric data, which are then fitted to mathematical models for diffusion and/or reaction. These models are inferential, as concentration profiles in the system have not been measured directly. The resulting models are consequently of limited complexity and involve little physical insight. The situation of diffusion and reaction in cereal grains is analogous to that found within porous catalyst pellets. Heterogeneous catalysis involves reactions which occur rapidly on the pore surfaces, the majority of which lie inside the pellet; thus often the rate-limiting step is diffusive. Optimizing catalyst efficiency requires a thorough knowledge of both the mass transport and reaction mechanisms involved, and extensive research has been undertaken by the chemical industry to understand these mech-

Table 1. Summary of Previous Grain Cooking Models

Author	Material	Exp.	Model	Ref. Temp. (°C)*	Activation Energy (kJ·mol^{-1})	
					< Ref. Temp.	> Ref. Temp.
Fan et al. (1961)	Wheat-Ponca	M	i	65	47	80
	Wheat-Vernum	M	i	65	42	69
	Wheat-Seneca	M	i	65	43	60
	Wheat-Brevor	M	i	65	49	73
Bandyopadhyay and Roy (1976)	Padma rice	M	i	68	31	133
	Jaya rice	M	i	63	32	106
	Ratna rice	M	i	62	18	107
Suzuki et al. (1976)	Tropical milled rice	P	ii	110	80	37
	Tropical milled rice	M	iii-react	110	67	Data Not
			iii-diff	110	37	Quoted
Suzuki et al. (1977)	Tropical milled rice	M	iii-react	50	2.1	84
			iii-diff	50	11.4	Varies
Cho et al. (1980)	Milyang rice	M	i	40	24	N/A
	Akibare rice	M	i	40	17	N/A
	Milyang rice	H	ii	100	78	36
	Akibare rice	H	ii	100	72	40
Bakshi and Singh (1980)	Rough rice	I	ii	85	77	103
	Brown rice	I	ii	85	44	40
	Rough rice	M	iv-D	85	33	66
			iv-k	85	78	43.8
	Brown rice	M	iv-D	85	16	65
			iv-k	85	103	40
Cabrera et al. (1984)	Corn	I	ii	N/A	80	N/A
	Corn	M	iv-D	N/A	57	N/A
			iv-k		75	
Juliano and Perez (1986)	Tropical milled rice	H	ii	90	76–121	32–57

M = moisture uptake data; P = parallel plate plastometer; H = hardness testing; I = iodine value.
*Ref temp refers to the point on the Arrhenius plot where the slope (activation energy) appears to change.

anisms (see Haynes, 1988). As with cereal grain processing, the methods used to study these systems have traditionally been gravimetric. In recent years, however, new imaging techniques such as MRI have allowed the direct visualization of the processes taking place inside catalyst pellets (such as Hollewand and Gladden, 1993, 1995b). The technique maps the presence of nuclei of a particular isotope, most commonly hydrogen ^{1}H. Typical in-plane spatial resolution of 30 μm is possible. The experiment fails to detect molecules that are in a "solid" state (that is, immobile) as nuclei which are held stationary relax several orders of magnitude faster than the time scale of the experiment. That the signal arising is due solely to mobile "liquid" components is useful for studies of liquids diffusing through a solid material.

Here, we have employed the same methods used to study liquid migration in catalyst pellets and also polymers (Hyde et al., 1995) to image moisture distribution in wheat grains. Uncooked cereal grains have been imaged by other workers: Eccles et al. (1988) and Jenner et al. (1988) have mapped water diffusivity and velocity in raw grains, and Ruan et al. (1992) have imaged water penetrating into corn kernels at room temperature. Here, we are probing moisture diffusion at much higher temperatures (100°C and 120°C) by taking images of individual grains that have been cooked for different times, and quenched in cold water.

Use of PGSE NMR to measure self-diffusion

NMR also allows self-diffusion of molecules to be studied using the pulsed gradient spin-echo (PGSE) method (Stejskal and Tanner, 1965; see also Kärger et al., 1988). In PGSE NMR, the output signal is made sensitive to the movement of water molecules over a defined time period. This can be used to quantify the self-diffusion coefficient for unrestricted single component systems directly using

$$\ln \psi = D\gamma^2 g^2 \delta^2 \left(\Delta - \frac{\delta}{3}\right) \tag{2}$$

where ψ is signal attenuation; D is the self-diffusion coefficient ($m^2 \cdot s^{-1}$); γ is the gyromagnetic ratio (a constant for a given isotope) ($rad \cdot s^{-1} \cdot T^{-1}$); δ is the duration of applied magnetic field gradient (s); and g is the magnetic field gradient ($T \cdot m^{-1}$).

For liquids, it is found that a plot (henceforth referred to as the PGSE plot) of $\ln \psi$ vs. $\gamma^2 g^2 \delta^2 (\Delta - \delta/3)$ yields a straight line of gradient D. Deviations from linearity can be found in multicomponent systems or where diffusion is restricted. It is possible to model the PGSE response of a variety of idealized diffusion regimes and compare with experimental results.

The type of information gained from PGSE NMR thus contrasts with that gained from MRI, where diffusion is elucidated by comparing a sequence of images with computer models. PGSE, on the other hand, measures self-diffusion directly rather than diffusion down concentration gradients. Both methods have their shortcomings. With MRI, more than one diffusion scheme might explain the water distributions observed. Changes in the water activity coefficient, and the presence of restricting barriers (such as cell walls) can cause diffusivities measured by PGSE NMR to be unrepresentative of bulk diffusion (see Stapley et al., 1995). Since the two techniques provide different information, their combination can prove useful in building up an overall picture of the diffusion process. This approach has been used successfully to probe diffusion within catalyst pellets (Hollewand and Gladden, 1995a,b).

Experimental Studies

MRI analysis of boiled grains

Full details of the method and of the images are given in Stapley (1995) and Stapley et al. (1997a). Samples of Riband variety grains of mass between 35 and 40 mg were cooked either at 1 bara (c. 100°C) or 2 bara (c. 120°C) in a steam pressure cooker. Immediately after removal from the cooker, samples were quenched in cold water. After removal of surface moisture, grains were wrapped in a Teflon film to prevent moisture loss and transferred to a sample tube. Grains were imaged within 3 h of cooking. Moisture contents were obtained by weighing before and after cooking. The initial grain moisture contents (mc_o) were assumed the same for all the grains in the batch. Moisture contents from individual grains showed little variation (commonly about 10% mc_{wb} with a standard deviation of 0.7% mc_{wb}). For each batch, the initial moisture content was measured by vacuum drying a set of approximately 100 grains.

Imaging was performed using either Bruker MSL200 and Bruker DMX200 spectrometers; gradient strengths were typically 7 $G \cdot cm^{-1}$ using the MSL200 spectrometer and 40 $G \cdot cm^{-1}$ using the DMX200. In all cases the spin-echo technique was used with an echo time (T_E) of 2.2 ms and a repetition time (T_R) of 2 s. The internal diameter of the imaging probes was 5 mm. The slice selection gradient was chosen to yield a slice thickness of $\sim$0.8 mm in both cases. The field-of-view (corresponding to 128 pixels) of the images was 4.7 mm; thus, the inplane pixel resolution was 37 μm. The images shown here were taken with transverse slices through the center of the grain (across, rather than along the crease). Prior to image acquisition, the homogeneity of the receiver in the field-of view was checked by imaging a phantom of water. There is some weighting in the images due to T_2 relaxation. A number of methods were considered to correct for this (Stapley, 1995). A simple calibration from values of average pixel intensities vs. measured moisture contents, however, was the most reliable.

Data are presented here for experiments at 1 bara (about 100°C). Transverse images are shown in Figure 2. One-dimensional (1-D) concentration profiles were also extracted from the images along lines defined in Figure 3. Profiles along the line "C2" are shown in Figure 4. The data show water penetrating evenly into the grain from all points on the outer boundary, and, more slowly, from the inside of the crease. Results of experiments at 2 bara (about 120°C) showed similar behavior (Stapley, 1995; Stapley et al., 1997a). The concentration profiles can be characterized by a high moisture outer "plateau" region where the concentration varies only slightly, and an inner core, where the concentration varies markedly, dropping from the high moisture content of the "plateau" to a low moisture content at the grain center. Separating these two regions is a well defined "front," which moves towards the center of the grain as cooking proceeds.

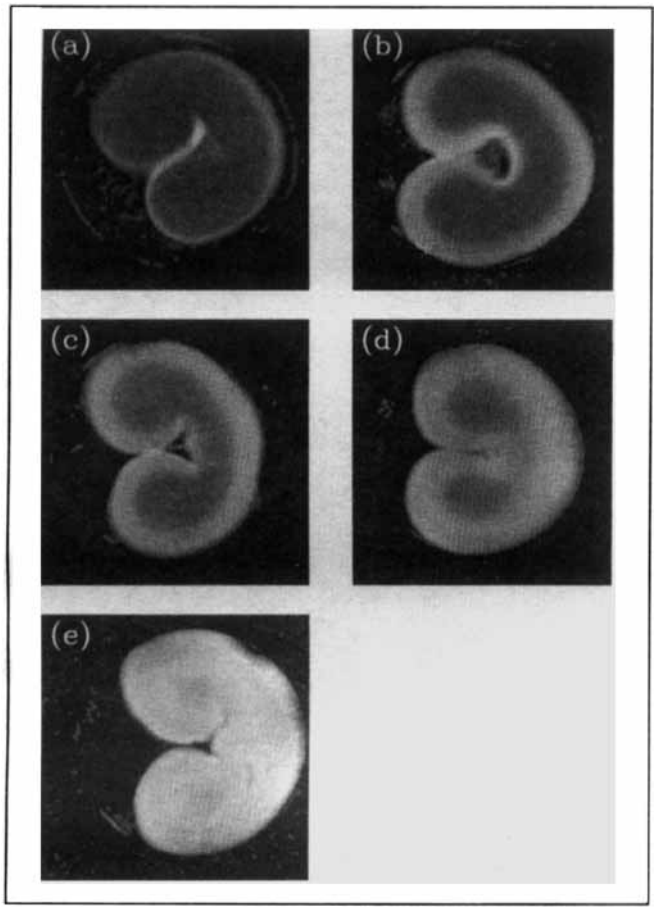

Figure 2. Corrected NMR images of moisture content for grains boiled in distilled water at 1 bara (~ 100°C) for (a) 5 min, (b) 10 min, (c) 15 min, (d) 20 min, and (e) 30 min.

Moisture content scale runs from 70% (white) to 0% (black), and the field-of-view is 4.7 mm (pixel resolution = 37 μm).

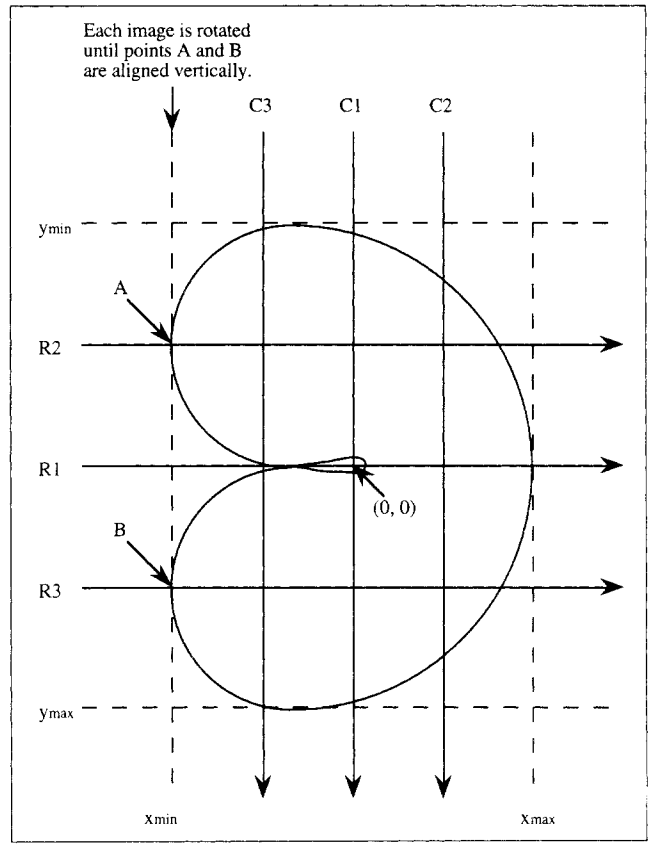

Figure 3. Location of profiles.

Images were first rotated until the grain cheeks were aligned as above (points A and B vertically aligned). Maximum and minimum x and y values were then established, and three profiles in each direction were extracted equally spaced between these limits.

The moisture content in the "plateau" region also rises during cooking.

Measurement of the self-diffusion of water in wheat grains

PGSE experiments were performed on whole wheat grains processed by soaking or boiling at a variety of moisture contents. Boiled grains were fully processed for 15 min at 2 bara, and soaked grains were immersed in water for 24 h. Samples were then dried to the requisite moisture content and then allowed to equilibrate overnight. Any grains found to have begun to germinate were discarded. Typically two to four nominally identical grains ($\pm 1\%$ *mc*) were used in a PGSE experiment to increase the signal-to-noise ratio. Moisture contents were calculated gravimetrically, grains typically lost 1% *mc* during the NMR experiment.

NMR measurements were performed using a Bruker MSL 200 at 20°C using the stimulated echo PGSE technique (see Kärger et al., 1988), with a Bruker Z32FHP-DIFF 200WB ^{1}H 7.5 probe and a Bruker B-Z 18B gradient unit. For each sample, the pulse sequence was performed for different gradient pulse time (δ) and diffusion times (Δ) (20, 100, and 400 ms), and the resulting echo amplitude was recorded. The unattenuated echo amplitude was measured using a very short gradient time, so that the attenuations measured were a direct result of increasing the gradient pulse time. Gradient strengths were typically 170 or 200 G·cm^{-1}. The time interval between the first r.f. pulse and first field-gradient pulse

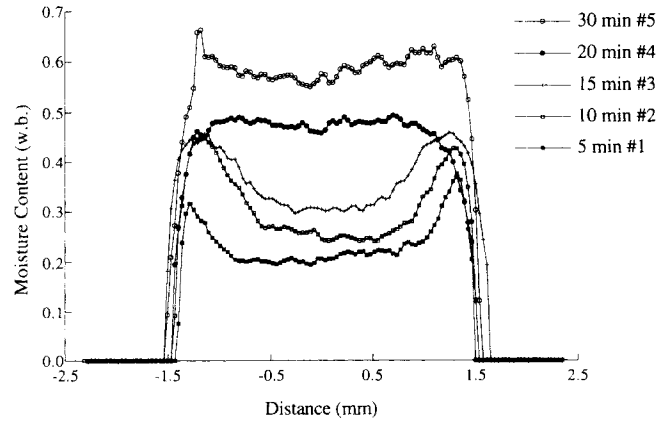

Figure 4. Corrected NMR profiles (from profile C2) of moisture content for grains boiled in distilled water at 1 bara (~ 100°C).

Profiles are labeled with the nominal cooking times.

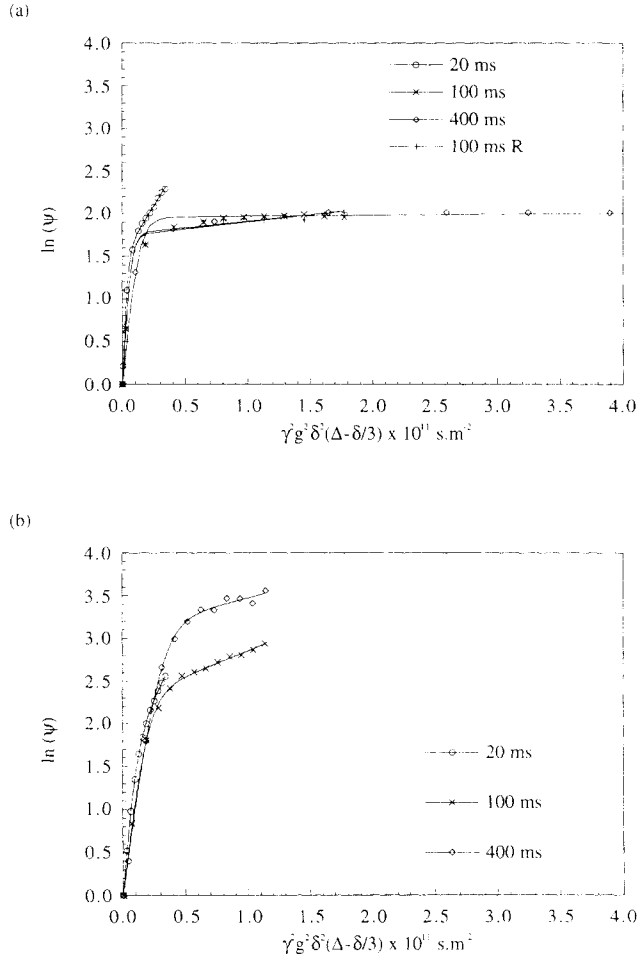

Figure 5. PGSE data taken at various diffusion times Δ (20, 100 and 400 ms) along with fits to the two component model (solid line).

(a) Soaked grains of moisture content 37.7%, and (b) grains boiled for 15 min in distilled water at 2 bara (~ 120°C) and then dried to a moisture content of 37.3% (R = repeat measurements).

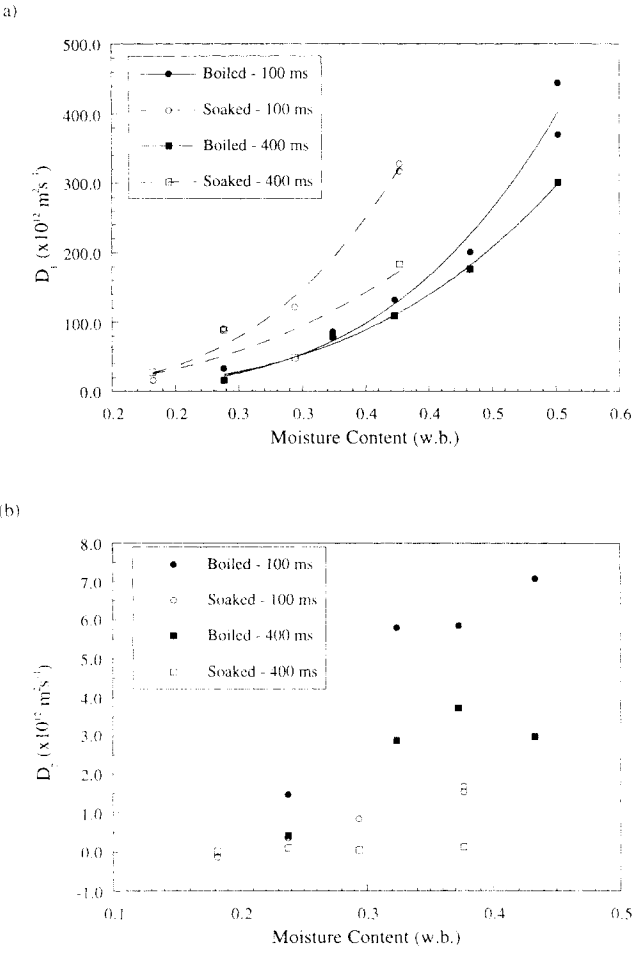

Figure 6. Variation of (a) fit parameter D_1, and (b) fit parameter D_2 with grain moisture content for soaked and boiled grains for PGSE experiments with a diffusion time of 100 ms and 400 ms.

Curve is a fit to data of Eq. 4.

was 1 ms, and the interval between the first and second r.f. pulses was 5 ms.

Sample PGSE plots are shown in Figures 5a and 5b for soaked and boiled grains at a moisture content of circa 37%. The plots are generally nonlinear showing an initial steep line followed by a much flatter asymptote. There was a marked difference between PGSE plots for cooked and uncooked grains. Uncooked grains gave a horizontal asymptote, whereas any asymptotes observed with cooked grains were sloping.

The data best fitted a two-component model for diffusion, where two pools of different diffusivities D_1 and D_2 contribute fractions p and $(1-p)$ to the observed signal (component 1 is that with the higher diffusivity)

$$\frac{1}{\psi} = p\cdot\exp\left[-D_1\gamma g\delta\left(\Delta-\frac{\delta}{3}\right)\right] + (1-p)\cdot\exp\left[-D_2\gamma g\delta\left(\Delta-\frac{\delta}{3}\right)\right] \quad (3)$$

The variation of D_1 and D_2 with moisture content is shown in Figures 6a and 6b. D_1 appears to be a strong increasing function of moisture content. Maximum values measured ($\sim 3\times10^{-10}$ m$^2\cdot$s^{-1} at 50% moisture content) were approximately one-sixth that of pure water (2×10^{-9} m$^2\cdot$s^{-1}). A power law relationship was found to describe satisfactorily the data for D_1

$$D_1 = D_0(mc_{wb})^n \quad (4)$$

Fitted values for D_0 and n are shown in Table 2. D_2 values are significantly lower, and do not appear to be a strong function of moisture content. There is, however, an order of magnitude difference in D_2 values for cooked and uncooked grains (averaging $\sim 1\times10^{-13}$ m$^2\cdot$s^{-1} for soaked grains, and $\sim 30\times10^{-13}$ m$^2\cdot$s^{-1} for cooked grains, see Table 2). This is related to the different slopes of the asymptotes observed. The plots show only a limited dependence on diffusion time indicating that diffusion is not significantly restricted on the micron length scale (the maximum length scale probed was

Table 2. Results of Fits of PGSE Data to Two-Component Model

Grain Treatment	Diffusion Time, Δ (ms)	Component 1 Data $D_0 \times (10^{-13}\ m^2 \cdot s^{-1})$	Component 1 Data n	Component 2 Data $D_2 \times (10^{-13}\ m^2 \cdot s^{-1})$
Soaked	100 ms	9,040 ± 3,430	3.42 ± 0.38	0.86 ± 0.77
	400 ms	5,940 ± 2,340	3.90 ± 0.54	0.07 ± 0.05
Boiled	100 ms	2,310 ± 3,060	2.65 ± 1.23	22.6 ± 27.4
	400 ms	3,060 ± 430	3.37 ± 0.18	5.6 ± 7.0

ca. 15 μm). There does appear to be some effect of diffusion time on D_2, suggesting that diffusion is more restricted for that component.

The nature of the two components is unclear from these experiments as one cannot measure the relative proportions of the two components without a knowledge of their NMR relaxation behavior. It is possible that component 1 refers to intergranular water (or possibly water in the bran layers) and component 2 is water within the starch granule. This would explain the more restricted diffusion and slower diffusion rates of component 2 and the higher variation of D_1 with moisture content. The D_1 values are lower than those found by Callaghan et al. (1979) (1.8×10^{-10} $m^2\cdot s^{-1}$ to 1.2×10^{-9} $m^2\cdot s^{-1}$ at 22°C). The data were obtained, however, with a much smaller diffusion time (6 ms). Callaghan et al. interpreted the results as diffusion through a randomly oriented array of capillaries. Eccles et al. (1988) combined the PGSE sequence with MRI and imaged the diffusion coefficient within wheat grains. Values between 5×10^{-10} $m^2\cdot s^{-1}$ and 10×10^{-10} $m^2\cdot s^{-1}$ were found (diffusion time was 5 ms). Van den Berg (1981, 1984), studying moisture sorption isotherms of wheat, also categorized the water population into a two-component model. This consisted of a strongly bound relatively immobile component which predominated at low moisture, and a more mobile component which increased in relative proportion as moisture contents were increased.

The two types of diffusion behavior observed here ("power law" observed with component 1 and the "step change" between uncooked and cooked material observed with component 2) are now incorporated into the finite-element model described in the next section, to be tested against the results of the MRI experiments.

Modeling

Comparison of boiling and steaming processes

The MRI experiments have shown that during boiling, water penetrates into the grain as a well-defined moisture front with a marked difference between the moisture content near the surface and at the center of the grain. These results are in marked contrast to the development of moisture profiles during steam cooking, which are essentially uniform. Heat transfer also plays an important part in wheat grain steaming, as condensing steam releases latent heat which must be conducted away (Stapley et al., 1998). This is not the case with boiling, where, except for the first few seconds of cooking, the grain is always at the temperature of the boiling water. An entirely different approach is thus required to model the two processes. For boiling, it is not necessary to solve equations for heat transfer to predict the temperature distribution within the grain. It is, however, necessary to develop a model for water motion within the grain.

Modeling Wheat Grain Boiling

The finite-element method (FEM) was employed to model grain boiling as it can cope with both the unusual shape of the wheat grain and complicated expressions for the diffusion coefficient. Simulations can also be compared directly with the MRI data. The method has found useful applications in many areas of food processing, despite the amount of computing power required (Puri and Anantheswaran, 1993). 3-D simulation was not attempted as it was assumed that the central slice is a plane of symmetry within the wheat grain (ignoring the wheat germ), so flows within that area are 2-D and in the plane of the slice. It was further assumed that the central slice is itself symmetric along the line of the crease. The NMR images in Figure 2 show that this is not always strictly true; but this approximation significantly reduces the complexity of the computation. The following scheme was used:

(i) One-dimensional Cartesian models were used for initial fitting of data. 2-D models (using the shape of a central slice of the wheat grain cross section) were then performed to give more detailed fitting to the NMR images.

(ii) Meshes consisted of 25 elements and 51 nodes for the 1-D formulation, and 1,440 elements and 769 nodes for the 2-D shape, using triangular elements.

(iii) 5 gauss points per element were used for 1-D problems, and just one gauss point for the 2-D mesh (to maximize stability for cases where large variations in diffusivity are expected across an element). Linear shape functions were used for both 1-D and 2-D problems.

(iv) To generalize the simulation and make it easier to compare results with experimental data, the diffusion equation was used in a nondimensional form, that is

$$\text{1-D:} \qquad \frac{\partial}{\partial z_1}\left(D^*\frac{\partial X}{\partial z_1}\right)=\frac{\partial X}{\partial \tau} \tag{5}$$

$$\text{2-D:} \qquad \frac{\partial}{\partial z_1}\left(D^*\frac{\partial X}{\partial z_1}\right)+\frac{\partial}{\partial z_2}\left(D^*\frac{\partial X}{\partial z_2}\right)=\frac{\partial X}{\partial \tau} \tag{6}$$

where

$$D^*=\frac{D}{D_0}, \quad X=\frac{c-c_0}{c_{sat}-c_0}, \quad z_1=\frac{x}{L},$$

$$z_2=\frac{y}{L}, \quad \tau=\frac{tD_0}{L^2}=\frac{t}{\epsilon}$$

D_0 is a constant ($m^2\cdot s^{-1}$); c_0 is the initial concentration or moisture content (w.b.); c_{sat} is the surface concentration or moisture content (w.b); L is the characteristic length, m; and ϵ is a constant, s.

(v) Time intervals were set to be as large as possible while providing a solution that is "accurate." Sufficient accuracy was assumed if, when the step size was halved, the result was not significantly different (less than 1%). Time-stepping using the Galerkin method ($\theta = 2/3$) was judged to be a sensible "com-

promise" between the various merits and drawbacks of explicit and implicit methods.

The finite-element code was tested by comparing solutions for 1-D diffusion (for both 1-D and 2-D finite-element formulations) with those presented by Carslaw and Jaeger (1959) for the mathematically equivalent case of heat conduction in rods.

Fitting model to MRI data

Ideally, the best way to fit data from an NMR image to a numerical model would be to take each pixel from the image and compare its intensity to the model prediction. However, this is computationally intensive, and the irregularities of the wheat grain shape make it difficult to superimpose the NMR images on the idealized grain shape used in the finite-element model. Instead, six representative profiles were taken from each image, as shown in Figure 3.

The nondimensionalized concentration and time scales used with the FEM obviously differ from the real concentrations and time scales of the NMR images. They are nonetheless linearly related and can be expressed using two fitting parameters, ϵ and mc_{sat} (saturation moisture content)

$$t = \epsilon\tau \tag{7}$$

$$mc_{wb} = mc_o + (mc_{sat} - mc_o)X \tag{8}$$

It was assumed (Stapley, 1995) that all grains possessed an initial moisture content (mc_o) of 10%, which corresponds to zero on the finite-element scale. Similarly, zero cook time was set equal to zero FEM time. Cook times were defined here as the time the grain spent in the cooker.

It is important to be able to associate an NMR data point with the corresponding coordinates on the FEM model to allow predicted FEM values to be identified and compared with the experiment. The first part of the procedure was to trim the NMR profiles so that pixels outside of the grain were not included in the analysis. The remaining pixels were then allocated FEM coordinates evenly along the FEM profile. Extracting the FEM value corresponding to these points requires interpolation, as only nodal values are explicitly given by the model. This first requires identifying which element contains the point in question. For the 1-D scheme, this is straightforward and a search is made for the element whose outermost node coordinates contain the data point. For 2-D elements, one must determine whether the data point lies within the three defining sides of a particular triangle. This was achieved using a vector product approach (Stapley, 1995). Once the correct element was found, the FEM value corresponding to the point in question was interpolated using the element shape functions. The FEM values were then compared with experimental data and optimum values of ϵ and mc_{sat} found. The fit procedure used two nested search algorithms (using Powell's method; Press et al., 1992) to find the optimum values of ϵ and mc_{sat}, which minimize the RMS difference between the NMR profiles from a series of images (for either 100°C or 120°C) and the corresponding FEM output. The RMS difference can be expressed as

$$\text{RMS} = \sqrt{\left(\sum_{\text{profile}} \left[mc_i - \left(0.1 + (mc_{sat} - mc_0)X_i\right)\right]^2 \right)} \tag{9}$$

The outer loop of the algorithm searches for mc_{sat}, and the inner loop for ϵ (varying ϵ affects which time steps of the FEM output are compared to each image). Fits were carried out using output from both 1-D and 2-D models. 1-D models were compared to profile "C2" only (defined in Figure 3), whereas 2-D models were compared with all six profiles (an average RMS value from the six profiles being taken as the quantity to be minimized). The fits produce three numbers: ϵ, mc_{sat} and the RMS difference between the NMR images and the FEM model. The value of mc_{sat} is the calculated saturation moisture content. The diffusion coefficient is calculated from ϵ, and the characteristic length L (taken as 3.75 mm) using Eq. 10

$$D_0 = \frac{L^2}{\epsilon} \tag{10}$$

Table 3. Results of Fits of the 1-D and 2-D FEM Models for Grain Boiling

Model	1-D/2-D	Process	Sat *mc*	ϵ (s)	$D_0 \times (10^{-10}\ \text{m}^2\cdot\text{s}^{-1})$	RMS Error	Notes
Fickian	1-D	1 bara	0.540	13,200	12.1	0.0617	
		2 bara	0.508	5,900	27.1	0.0577	
	2-D	1 bara	0.519	51,400	2.73	0.0647	
		2 bara	0.498	23,200	6.05	0.0685	
Power Law	1-D	1 bara	0.490	360	440	0.0787	$n = 3.5$
		2 bara	0.460	170	950	0.0602	$n = 3.5$
	2-D	1 bara	0.465	1,400	100	0.0805	$n = 3.5$
		2 bara	0.450	610	230	0.0735	$n = 3.5$
Step Change	1-D	1 bara	0.491	15,000	10.7	0.0603	$F = 30$; $X = 0.99$
		2 bara	0.442	8,200	19.6	0.0541	$F = 30$; $X = 0.98$
	2-D	1 bara	0.496	46,200	3.05	0.0603	$F = 30$; $X = 0.99$
		2 bara	0.477	20,800	6.77	0.0647	$F = 30$; $X = 0.99$
Thomas Windle Step Change	1-D	1 bara	0.500	30,800	4.57	0.0553	$F = 30$; $X = 0.99$; $K = 15$; $\Gamma = 5$
		2 bara	0.450	12,900	10.9	0.0403	$F = 30$; $X = 0.99$; $K = 15$; $\Gamma = 5$
	2-D	1 bara	0.541	34,400	4.09	0.0570	$F = 6$; $X = 0.95$; $K = 60$; $\Gamma = 1.0$
		2 bara	0.502	14,500	9.66	0.0562	$F = 6$; $X = 0.95$; $K = 40$; $\Gamma = 1.6$

Candidate models

A number of different model scenarios were tested to see how they fit the MRI data, using the RMS error values as a guide.

(i) Fickian Diffusion. $D^* = 1$. The diffusion coefficient is kept constant. This is the simplest model and as such acts as a benchmark. The fit yields a value of the diffusion coefficient D_0 from ϵ using Eq. 10.

(ii) Power Law Variation of Diffusion Coefficient with Moisture Content. The PGSE experiments with wheat grains (see earlier subsection) suggested that the diffusivity of a fraction of the water in wheat grains ("component 1") varies with moisture content according to a power law relation (see Eq. 4). This is expressed in nondimensionalized variables, as

$$D^* = [0.1 + (mc_{sat} - 0.1) \cdot X]^n \tag{11}$$

The value of n found from PGSE data was approximately 3.5, and this value was used in the simulations. It was necessary to provide an initial guess for mc_{sat} for the simulation to run. This was assumed to be 0.5, which proved satisfactory in most cases.

(iii) Step Change in Diffusivity. The PGSE experiments also suggested a second component of water in the grain. The data for this component indicated an increase in diffusivity of 6 to 30 times between cooked and uncooked grains for the same moisture content, possibly as a result of the starch moving through a glass transition. As cooking is essentially isothermal, the glass transition will occur solely as a result of increased moisture content. The model was therefore run applying a step-change in diffusivity of factor F at a critical (nondimensionalized) moisture content (X_{crit}), that is

$$\begin{aligned} D^* &= 1 \qquad \text{for } X < X_{crit} \\ D^* &= F \cdot \qquad \text{for } X \geq X_{crit} \end{aligned} \tag{12}$$

Optimum values of F and X_{crit} were found by a manual search for the combination which provided the least RMS error value.

(iv) Viscous Relaxation/Diffusion Model. The shapes of the profiles from the NMR images (Figure 4) are similar to those found in a number of other polymer systems (such as iodohexane in polystyrene; see Hui et al., 1987), in which diffusion is affected by the polymer changing from a glassy to a rubbery state at the front. Unlike conventional diffusion, the rate-limiting step of the process is often the glass transition itself, that is, the polymer chains take a finite time to relax and allow more water into the polymer matrix. The glass transition of starch is an established feature of the starch gelatinization process, and so starch systems may exhibit similar diffusive behavior.

This effect can be modeled, and the approach of Thomas and Windle (1982) has been adopted here. The Thomas-Windle model simultaneously solves for the solute activity and solute volume fraction using the following scheme (expressed here in 1-D)

$$\frac{\partial a}{\partial t} = \left(\frac{\partial a}{\partial \phi}\right) \frac{\partial}{\partial x}\left(D \frac{\phi}{a} \frac{\partial a}{\partial x}\right) \tag{13}$$

$$\frac{\partial \phi}{\partial t} = B \ln\left(\frac{a}{\phi}\right) \exp(m \cdot \phi) \tag{14}$$

where a is the solute activity; ϕ is the volume fraction of solute (approximately equivalent to moisture content); and B, m are constants.

The Thomas-Windle model has previously been used to model diffusion in synthetic polymers, and builds upon the diffusion equation by including an extra equation to describe the effect of polymer relaxation on mass transport. By varying the relaxation parameters (m and B), it is possible to model situations in between the extreme cases where diffusion is totally controlled by relaxation (Case II diffusion), or where relaxation has no effect (which can be modeled using the diffusion equation only). Most diffusion behavior in polymers falls between the linear-in-time kinetics of Case II behavior and the linear-in-square-root-of-time behavior of Fickian diffusion, in a third category termed "anomalous" diffusion. The two equations are solved simultaneously for a and ϕ, by alternately time-stepping each equation. Over a time step, the change in a is evaluated using Eq. 13 at a constant value of (a/ϕ), and the change in ϕ is given by Eq. 14 using a constant value of a.

Nondimensionalizing Eqs. 13 and 14 and using moisture content rather than volume fraction yields

$$\frac{\partial \alpha}{\partial \tau} = \frac{\partial \alpha}{\partial X} \frac{\partial}{\partial z_1}\left(D^* \left[\frac{mc_0 + X(mc_{sat} - mc_0)}{mc_0 + \alpha(mc_{sat} - mc_0)}\right] \frac{\partial X}{\partial z_1}\right) \tag{15}$$

$$\frac{\partial X}{\partial \tau} = K \ln\left[\frac{mc_0 + \alpha(mc_{sat} - mc_0)}{mc_0 + X(mc_{sat} - mc_0)}\right] \exp(\Gamma X) \tag{16}$$

where

$$K = \frac{Bx_0^2 \exp[mc_0 \cdot m]}{D_0(mc_{sat} - mc_0)} \tag{17}$$

$$\Gamma = m(mc_{sat} - mc_0) \tag{18}$$

$$\alpha = \frac{a - mc_0}{mc_{sat} - mc_0} \tag{19}$$

The diffusivity D is usually also made a function of moisture content. In the literature both step change (Hui et al., 1987) and exponential laws (Thomas and Windle, 1982) have been used. Here, a power law (model iv-a) and a step change relationship model (model iv-b) were used. The power law relationship was used rather than an exponential law as this type of relationship was indicated from the PGSE results. Simulations were run using both these relations for diffusivity. Different values of K and Γ were tested to minimize the RMS error value. When run with a step change in diffusivity, however, the optimization requires variation in four independent parameters to minimize the RMS error (F, X_{crit}, K and Γ), and thus requires a considerable number of simulations to obtain a global minimum. The values of F and X_{crit} for 1-D simulations were therefore fixed at the "best solution" found from the step-change model. Simulations using the 2-D model encountered some problems using this method, and it was found that more stable solutions were obtained with slightly lower values of X_{crit}.

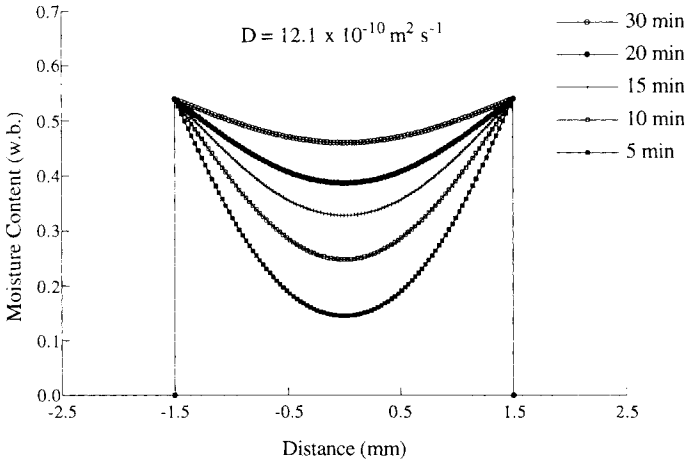

Figure 7. 1-D finite-element simulation for diffusion in wheat grains using a Fickian model (model (i)-constant diffusivity).

Profiles shown are the results of fits to data from profile C2 for grains boiled in distilled water at 1 bara (~ 100°C) (c.f. Figure 4).

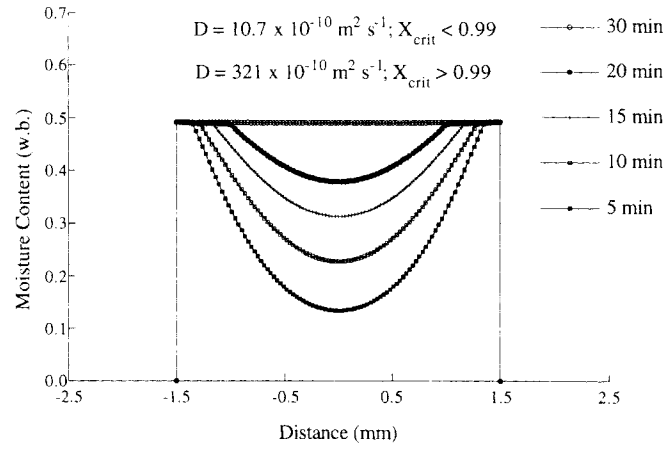

Figure 9. 1-D finite-element simulation for diffusion in wheat grains using a model where the diffusivity increases by a factor of 30 above a moisture content of 99% of the saturation value (model (iii)).

Profiles shown are the results of fits to data from profile C2 for grains boiled in distilled water at 1 bara (~ 100°C) (c.f. Figure 4).

Results

The results of the fits to the candidate models are presented in Table 3. 1-D profiles are shown in Figures 7 to 10 as they best show the nature of the moisture distributions arising. In general, smaller diffusion coefficients were obtained when the model was run in 2-D. This is attributed to the profile chosen for the 1-D fits (C2 in Figure 3) not running across the narrowest section for diffusion of the grain (rather it lies at an angle) resulting in an erroneous value of L, and that the fitted values of D_0 depend on the square of the value of L that is used.

(i) Fickian Diffusion. The fitted 1-D profiles are shown in Figure 7. The general form of the profiles is a series of "concave" curves which gradually rise with increasing time. It can be seen from Table 3 that the increase in temperature from 100°C to 120°C more than doubles the value of the fitted Fickian diffusion coefficient. The results of the fit of the 2-D model to the 1 bara data showed diffusivities similar to those reported by Fan et al. (1961), who also used a Fickian based model to fit to data for moisture uptake (see subsection on previous models of grain processing). Although the RMS error value of $\sim 0.06\%\ mc_{wb}$ indicates a reasonable fit to the data, the Fickian model does not predict the shape of the

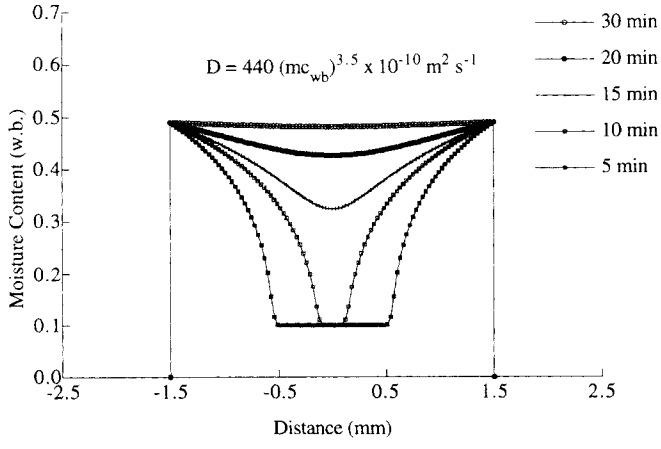

Figure 8. 1-D finite-element simulation for diffusion in wheat grains using a model where the diffusivity increases with moisture content according to a power law relation (model (ii)).

Profiles shown are the results of fits to data from profile C2 for grains boiled in distilled water at 1 bara (~ 100°C) (c.f. Figure 4).

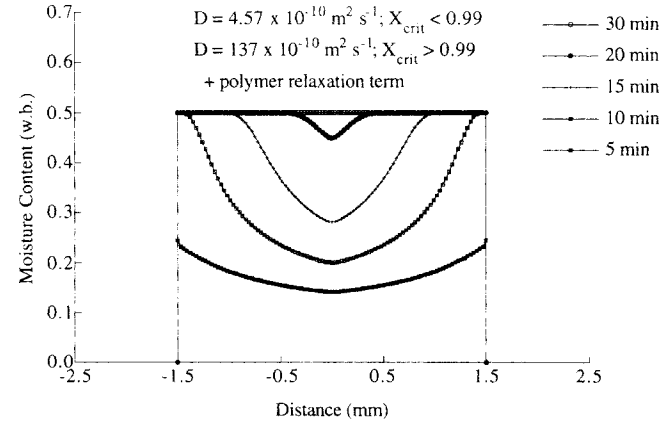

Figure 10. 1-D finite-element simulation for diffusion in wheat grains using the Thomas-Windle relaxation/diffusion model (with a step change in diffusivity of 30 at a moisture content of 99% of the saturation value, with values of K and Γ of 15 and 5, respectively (model (iv-b)).

Profiles shown are the results of fits to data from profile C2 for grains boiled in distilled water at 1 bara (~ 100°C) (c.f. Figure 4).

front observed on the NMR images, and thus does not completely describe the process.

(ii) Power Law Model. In contrast to the Fickian diffusion curves, the power law model (see Figure 8) results in a series of "convex" curves with the center line remaining constant at the initial concentration for more than 10 min into the simulation. These curves do not reflect the shape of the image profiles, and higher RMS values were found as a result.

(iii) Step-Change Model. The profiles for the step-change model (Figure 9) show the concave curves found with the Fickian diffusion model, together with a surface region where the concentration is above X_{crit} and within which the profiles are relatively flat. There is a discontinuity in slope between these two regions, which is expected to differ by the factor F where they meet (so that the flux of solute is maintained). The position of the discontinuity moves towards the center as time progresses. The profiles thus bear some resemblance to the NMR images as they possess both a "front" and concave profiles within the core. Consequently, the RMS error values are better than those of the purely Fickian diffusion model. Similar RMS values were found with other combinations of F and X_{crit} giving similar values of $F \cdot (1 - X_{crit})$ (a quantity proportional to the flux diffusing in at any time). Optimum values of X_{crit} were found to be just under the saturation value (0.99), with a step-change increase factor (F) of 30. Nevertheless, the model fixes the surface concentration at a constant value, whereas the NMR images show the surface concentration to increase during cooking.

(iv) Thomas-Windle Model. The results of the fit to data of the Thomas-Windle models with power law variation of diffusivity with moisture content (model (iv-a)) were poor. The RMS values are much higher for this model than other simulations, and some could not be fitted at all. This is due to the very sharp profiles that arose from the use of this model (which are typical of pure Case II diffusion). Such sharp profiles are inherent from a diffusivity law in which such large increases of diffusivity occur over the moisture content range. There remains a possibility that a "correct combination" of K and Γ may exist, but this was not found. This model is therefore rejected.

The results of the fit to data of the Thomas-Windle model with a step change in diffusivity (model (iv-b)) were the best of any of the models tested in both 1-D and 2-D simulations. The model is essentially an extension of model (iii) with the addition of two more fitting parameters, and this will clearly improve the fit obtained. This is manifested most clearly in the behavior of the surface concentration, which is allowed to slowly increase with time in the Thomas-Windle model, but is fixed in the purely diffusional models at the saturation value. The 1-D fitted profiles are shown in Figure 10, and the 2-D simulation results are shown in Figure 11. Both show good agreement with the MRI data.

Discussion and Conclusions

MRI has shown that, when cooking grains in boiling water, there is a large internal concentration gradient within the grain, and thus a significant internal mass-transfer resistance exists. The images are characterized by an incoming moisture front, although water does penetrate ahead of this front.

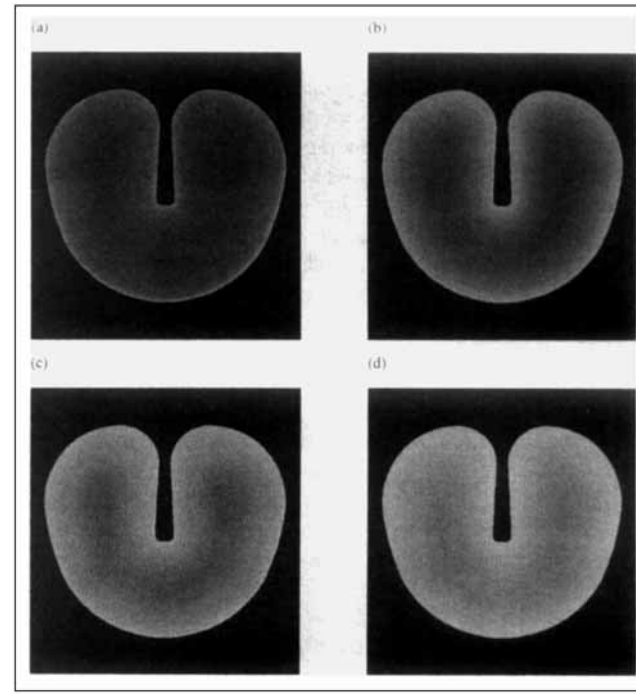

Figure 11. 2-D finite-element simulation for diffusion in wheat grains using the Thomas-Windle relaxation/diffusion model (with a step change in diffusivity of 6 at a moisture content of 95%, with values of K and Γ of 60 and 1.0, respectively (model (iv-b)).

Images shown are the results of fits to data from NMR images of grains boiled at 1 bara c. 100°C and correspond to cooking times of (a) 5 min, (b) 10 min, (c) 15 min, and (d) 20 min (c.f. Figure 2).

Pulsed gradient spin-echo NMR detected the presence of possibly two components of water within the grain: a fast-diffusing component whose diffusivity increased with moisture content (approximately power law variation), and a slower component whose diffusivity appears to be much larger with cooked grains than uncooked grains.

Boiling has been modeled, assuming isothermal conditions, using the finite-element method to solve equations for mass transfer within the grain based upon the diffusion equation. The output from 1-D and 2-D simulations was fitted to the profiles extracted from the NMR images of boiled grains. A number of candidate models have been tested against the imaging data:

(i) Fickian diffusion.

(ii) The "power-law" model for diffusion coefficients, a form suggested from PGSE NMR.

(iii) The "step-change" model, again suggested from the PGSE experiments.

(iv) The Thomas-Windle model (Eqs. 13 and 14), which incorporates the viscous relaxation effect of polymer chains on solute diffusion, combined with (ii) and (iii).

It was found that the diffusion coefficients fitted using any of the diffusion models tested are higher by more than a factor of two for boiling at 2 bara compared to boiling at 1 bara. This suggests an activation energy for the process of ca. 40

$kJ \cdot mol^{-1}$, although this number has only limited meaning considering the overall complexity of the process. Of the models tested, the best fits were obtained with the Thomas-Windle model with a step change in diffusivity (model iv-b), followed by the step change model (iii), the Fickian diffusion model (i), and the power law models (ii) and (iv-a). Thus, of the two types of diffusion behavior observed in the PGSE experiments, it is the step-change model which appears to control the actual behavior of the system. The moisture whose diffusion obeys the power law thus appears to represent either only a small component or a component not involved in any rate-limiting process.

The "step-change Thomas-Windle" model is particularly adept at simulating the surface concentration, which in reality rises slowly with time. This obviously cannot be modeled using the diffusion equation with a fixed concentration boundary condition, although such behavior could conceivably be achieved using a mass-transfer coefficient boundary condition (the mass-transfer resistance arising due to the presence of the pericarp).

The results of the fit to the Thomas-Windle model suggest that the diffusion lies in the so-called "anomalous" regime between purely Fickian and Case II diffusion. Both the anomalous and step-change natures of the fitted model have been observed for polymers going through a glass transition, which is widely believed to occur when a starch gelatinizes. Stapley et al. (1997b) found that the fraction of unconverted starch in partially boiled grains, as measured by DSC, decreases with cooking time at a rate commensurate with the speed of the incoming moisture front observed in the NMR images. Thus, it appears likely that this moisture front also represents a gelatinization front, dividing a rubbery outer region from an inner glassy core.

For the Riband type grains used in our experiments, it is now possible to accurately estimate both the moisture content and moisture distribution during processing. It is not known how appropriate the model predictions will be for other varieties or even grains of the same variety from different harvests. This will require confirmation from further studies. However, the polymeric basis of the Thomas-Windle model is a significant advance over previous grain cooking models in terms of the underlying science. The combination of this engineering understanding with a knowledge of texture and flavor aspects of the grain may well make novel products possible. A polymer diffusion approach may also be useful in probing other high-temperature starch systems such as extruded food products, and, on a subgranular level, even the gelatinization process itself.

Acknowledgments

AGFS would like to thank Weetabix Ltd. and the BBSRC for financial support. Discussions with John Pickles and Chris Hart of Weetabix Ltd. were invaluable throughout the project.

Notation

c = concentration
D^* = nondimensionalized diffusion coefficient
D_1 = diffusion coefficient of component 1 ($m^2 \cdot s^{-1}$)
D_2 = diffusion coefficient of component 2 ($m^2 \cdot s^{-1}$)
F = constant
k = rate constant (s^{-1})
n = power law constant
r = radial distance, m
t = time, s
x = distance, m
X = nondimensionalized concentration
z_1, z_2 = nondimensionalized distance
α = nondimensionalized activity
$\epsilon = L^2/D_0$
K, Γ = constants
τ = nondimensionalized time

Literature Cited

Bakshi, A. S., and R. P. Singh, "Kinetics of Water Diffusion and Starch Gelatinization during Rice Parboiling," *J. Food Sci.*, **45**, 1387 (1980).

Bakshi, A. S., and R. P. Singh, "Modelling Rice Parboiling Process," *Lebensm.-Wiss. u.-Technol.*, **15**, 89 (1982).

Bandyopadhyay, S., and N. C. Roy, "Kinetics of Absorption of Liquid Water by Paddy Grains during Parboiling," *Indian J. Tech.*, **14**, 27 (1976).

Becker, H. A., "A Study of Diffusion in Solids of Arbitrary Shape, with Application to the Drying of the Wheat Kernel," *J. Appl. Poly. Sci.*, **1**, 212 (1959).

Becker, H. A., "On the Absorption of Liquid Water by the Wheat Kernel," *Cereal Chem.*, **37**, 309 (1960).

Biliaderis, C. G., "Thermal Analysis of Food Carbohydrates," *Thermal Analysis of Foods*, V.R. Harwalkar and C.-Y. Ma, eds., p. 168 (1990).

Blanshard, J. M. V., "Starch Granule Structure and Function: a Physicochemical Approach," *Starch: Properties and Potential, Critical Reports on Applied Chemistry*, Vol. 13, T. Galliard, ed., Wiley, Chichester, U.K. (1987).

Cabrera, E., J. C. Pineda, C. Duran de Bazua, J. S. Segurajauregui, and E. J. Vernon, "Kinetics of Water Diffusion and Starch Gelatinization During Corn Nixtamilization," *Engineering and Food: Vol. 1. Engineering Sciences in the Food Industry*, p. 117 (1984).

Callaghan, P. T., K. W. Jolley, and J. Lelièvre, "Diffusion of Water in the Endosperm Tissue of Wheat Grains as Studied by Pulsed Field Gradient Nuclear Magnetic Resonance," *Biophysical J.*, **28**, 133 (1979).

Carslaw, H. S., and J. C. Jaeger, *Conduction of Heat in Solids*, 2nd ed., Clarendon Press, Oxford (1959).

Cho, E.-K., Y.-R. Pyun, S.-K. Kim, and J.-H. Yu, "Kinetic Studies on Hydration and Cooking of Rice," *Korean J. Food Sci. Tech.*, **12**, 285 (1980).

Danckwerts, P. V., "Absorption by Simultaneous Diffusion and Chemical Reaction," *Trans. Farad. Soc.*, **46**, 300 (1950).

Danckwerts, P. V., "Absorption by Simultaneous Diffusion and Chemical Reaction into Particles of Various Shapes and into Falling Bodies," *Trans. Farad. Soc.*, **47**, 1014 (1951).

Donovan, J. W., "Phase Transition of the Starch-Water System," *Biopolymers*, **18**, 263 (1979).

Eccles, C. D., P. T. Callaghan, and C. F. Jenner, "Measurement of the Self-diffusion Coefficient of Water as a Function of Position in Wheat Grain using Nuclear Magnetic Resonance," *Biophys. J.*, **53**, 77 (1988).

Eliasson, A.-C., "Effect of Water Content on the Gelatinization of Wheat Starch," *Starch/Stärke*, **32**, 270 (1980).

Fan, L. T., D. S. Chung, and J. A. Shellenberger, "Diffusion Coefficients of Water in Wheat Kernels," *Cereal Chem.*, **38**, 540 (1961).

French, D., "Organisation of Starch Granules," *Starch: Chemistry and Technology*, 2nd ed., R. L. Whistler, J. N. Bemiller and E. F. Pascall, eds., Academic Press, Orlando, p. 183 (1984).

Galliard, T., and P. Bowler, "Morphology and Composition of Starch," *Starch: Properties and Potential., Critical Reports on Applied Chemistry*, Vol. 13, T. Galliard, ed., Wiley, Chichester, U.K. (1987).

Haynes, H. W., "The Experimental Evaluation of Catalyst Effective Diffusivity," *Catal. Rev. Sci. Eng.*, **30**, 563 (1988).

Hollewand, M. P., and L. F. Gladden, "Heterogeneities in Structure and Diffusion within Porous Catalyst Support Pellets Observed by NMR Imaging," *J. Catal.*, **144**, 254 (1993).

Hollewand, M. P., and L. F. Gladden, "Transport Heterogeneity in

Porous Pellets: 1. PGSE NMR Studies," *Chem. Eng. Sci.*, **50**, 309 (1995a).
Hollewand, M. P., and L. F. Gladden, "Transport Heterogeneity in Porous Pellets: 2. NMR Imaging Studies under Transient and Steady-State Conditions," *Chem. Eng. Sci.*, **50**, 327 (1995b).
Hui, C. Y., K.-C. Wu, R. C. Lasky, and E. J. Kramer, "Case-II Diffusion in Polymers: II. Steady-State Front Motion," *J. Appl. Phys.*, **61**, 5137 (1987).
Hyde, T. M., L. F. Gladden, M. R. Mackley, and P. Gao, "Quantitative Nuclear Magnetic Resonance Imaging of Liquids in Swelling Polymers," *J. Poly. Sci. A*, **33**, 1795 (1995).
Imberty, A., A. Buléon, V. Tran, and S. Pérez, "Recent Advances in Knowledge of Starch Structure," *Starch/Stärke*, **43**, 375 (1991).
Jane, J.-L., T. Kasemsuwan, S. Leas, H. Zobel, and J. F. Robyt, "Anthology of Starch Granule Morphology by Scanning Electron Microscopy," *Starch/Stärke*, **46**, 121 (1994).
Jenner, C. F., Y. Xia, C. D. Eccles, and P. T. Callaghan, "Circulation of Water Within the Wheat Grain Revealed by Nuclear Magnetic Resonance Micro-Imaging," *Nature*, **336**, 399 (1988).
Juliano, B. O., and C. M. Perez, "Kinetic Studies on Cooking of Tropical Milled Rice," *Food Chem.*, **20**, 97 (1986).
Kärger, J., H. Pfeifer, and W. Heink, "Principles and Applications of Self Diffusion Measurements by Nuclear Magnetic Resonance," *Advances in Magnetic Resonance*, Vol. 12, W. S. Warren, ed., Academic Press, New York, p. 1 (1988).
Levine, H., and L. Slade, "Influences of the Glassy and Rubbery States on the Thermal, Mechanical, and Structural Properties of Doughs and Baked Products," *Dough Rheology and Baked Product Texture*, H. Faridi and J. M. Faubion, eds., Van Nostrand Reinhold, New York, p. 157 (1989).
Mattern, P. J., "Wheat," *Handbook of Cereal Science and Technology*, K. J. Lorenz and K. Kulp, eds., Marcel Dekker, New York (1991).
Miller, R. C., "Continuous Cooking of Breakfast Cereals," *Cereal Foods World*, **33**, 284 (1988).
Orth, R. A., and J. A. Shellenberger, "Origin, Production, and Utilization of Wheat," *Wheat: Chemistry and Technology*, 3rd ed., Vol. 1, Y. Pomeranz, ed., Amer. Assoc. Cereal Chemists (1988).
Press, W. H., S. A. Teukolsky, W. T. Vetterling, and B. P. Flannery, *Numerical Recipes in Fortran*, Cambridge University Press, Cambridge, UK, p. 406 (1992).
Puri, V. M., and R. C. Anantheswaran, "The Finite-Element Method in Food Processing: A Review," *J. Food Eng.*, **19**, 247 (1993).
Ruan, R., J. B. Litchfield, and S. R. Eckhoff, "Simultaneous and Nondestructive Measurement of Transient Moisture Profiles and Structural Changes in Corn Kernels During Steeping Using Microscopic Nuclear Magnetic Resonance Imaging," *Cereal Chem.*, **69**, 600 (1992).
Slade, L., and H. Levine, "Non-Equilibrium Melting of Native Granular Starch: I. Temperature Location of the Glass Transition Associated with Gelatinization of A-Type Cereal Starches," *Carbohydr. Poly.*, **8**, 183 (1988).
Stapley, A. G. F., "Diffusion and Reaction in Wheat Grains," PhD Thesis. University of Cambridge (1995).
Stapley, A. G. F., J. A. Sousa Gonçalves, M. P. Hollewand, L. F. Gladden, and P. J. Fryer, "An NMR Pulsed Field Gradient Study of the Electrical and Conventional Heating of Carrot," *Int. J. Food Sci. Technol.*, **30**, 639 (1995).
Stapley, A. G. F., T. M. Hyde, L. F. Gladden, and P. F. Fryer, "NMR Imaging of the Wheat Grain Cooking Process," *Int. J. Food Sci. Technol.*, **32**, 355 (1997a).
Stapley, A. G. F., L. F. Gladden, and P. J. Fryer, "A DSC Study of Wheat Grain Cooking," *Int. J. Food Sci. Technol.*, **32**, 473 (1997b).
Stapley, A. G. F., K. A. Landman, C. P. Please, and P. J. Fryer, "Modelling the Steaming of Whole Wheat Grains," *Chem. Eng. Sci.*, in press (1998).
Stejskal, E. O., and J. E. Tanner, "Spin Diffusion Measurements: Spin Echoes in the Presence of a Time-Dependent Field Gradient," *J. Chem. Phys.*, **42**, 288 (1965).
Stenvert, N. L., and K. Kingswood, "The Influence of the Physical Structure of the Protein Matrix on Wheat Hardness," *J. Sci. Fd. Agric.*, **28**, 11 (1977).
Suzuki, K., K. Kubota, M. Omichi, and H. Hosaka, "Kinetic Studies on Cooking of Rice," *J. Food Sci.*, **41**, 1180 (1976).
Suzuki, K., M. Aki, K. Kubota, and H. Hosaka, "Studies on the Cooking Rate Equations of Rice," *J. Food Sci.*, **42**, 1545 (1977).
Thomas, N. L., and A. H. Windle, "A Theory of Case II Diffusion," *Polymer*, **23**, 529 (1982).
van den Berg, C., "Vapour Sorption Equilibria and other Water-Starch Interactions; a Physico-chemical Approach," PhD Thesis. Agricultural Univ., Wageningen (1981).
van den Berg, C., "Description of Water Activity of Foods for Engineering Purposes by Means of the G.A.B. Model of Sorption," *Enginnering and Food Vol. 1-Engineering Sciences in the Food Industry*, B. M. McKenna, ed., Elsevier, London. p. 311 (1984).
Yaylayan, V., J. Fichtali, and F. R. van de Voort, "Production of Maillard Reaction Flavor Precursors by Extrusion Processing," *Food Res. Int.*, **25**, 175 (1992).

Manuscript received Jan. 15, 1998, and revision received May 4, 1998.